

VLSI IMPLEMENTED DATA-AIDED ML PARAMETER ESTIMATORS OF PSK BURST MODEMS

Yimin Jiang*, Wen-Chun Ting*, Farhad B. Verahrami*, Robert L. Richmond*, John S. Baras+

* Hughes Network Systems, Inc, 11717 Exploration Lane
 Germantown, MD 20876, E-mail: yjiang@hns.com
 + Institute for Systems Research, University of Maryland
 College Park, MD 20742, E-mail: baras@isr.umd.edu

ABSTRACT

A high performance Universal Modem ASIC that supports several modulation types and burst mode frame formats is under development. The ASIC is designed to work under stringent conditions such as large carrier frequency offset (up to 13% symbol rate) and low signal-to-noise ratio (SNR). Powerful and generic data-aided (DA) parameter estimators are necessary to accommodate many modes. In this paper we present an approximated maximum likelihood (ML) carrier frequency offset estimator, ML joint carrier phase and timing offsets estimator and their systolic VLSI implementations for PSK burst modems. The performances are close to the Cramer-Rao lower bounds (CRLB) at low SNRs. Compared with theoretical solutions the estimators proposed here are much simpler and easier to implement by the current VLSI technology.

1. INTRODUCTION

A high performance ASIC supporting Hughes Network System's Universal Modem product line is under development. This ASIC supports a variety of bit rates, modulations (BPSK, QPSK, 8PSK, OQPSK), forward error correction, and frame formats. In order to satisfy the stringent operating conditions such as large carrier frequency offset (up to 13% symbol rate), low SNR (E_b/N_0 around 0dB) and multiple operating modes, powerful and generic estimators are necessary to recover the burst parameters. Maximum likelihood (ML) estimators [5] are optimal estimators. We present a good approximation of DA ML carrier frequency offset estimator, a joint carrier phase and timing offsets estimator and their corresponding systolic [8] VLSI implementations.

Several carrier frequency offset estimation methods are discussed in [3]. The optimal ML frequency estimator is well known to be given by the location of the peak of a periodogram [9]. However the computation requirements make this approach prohibitive even with an FFT implementation. Therefore simpler approximation methods are desired. We present a DA carrier frequency offset estimator that is based on autocorrelation

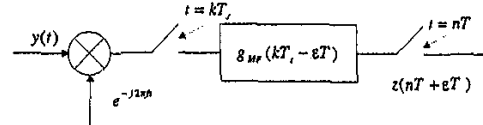


Figure 1: Matched Filter of Optimal Receiver

and the algorithm derived by Kay [2].

The DA ML joint carrier phase and timing offset estimator is derived in [1] (p.296). The presented implementation is hardware intensive. We derived a simplified ML joint carrier phase and timing offsets estimator, which is suitable for systolic VLSI implementation.

In section II the estimation algorithms are presented. Section III presents their efficient VLSI implementations. In the last section the CRLB_{DA} (for DA case) are investigated; the performance of the estimators is shown through computer simulation and compared with CRLB_{DA}.

2. ESTIMATION ALGORITHMS

The baseband received signal is modeled as:

$$y(t) = \sqrt{E_s} \sum_{n=0}^{N-1} [(a_{In}g(t-nT) + ja_{Qn}g(t-nT - \tau T)) \exp[j(2\pi ft + \theta)]] + n(t) \quad (1)$$

where $g(t) = g_T(t) \otimes c(t) \otimes f(t)$, $g_T(t)$ is the transmitter shaping function, $c(t)$ is the channel response, $f(t)$ is the prefilter, $n(t)$ is the additive white Gaussian noise (AWGN) with two-sided power spectral density $N_0/2$, and $a_n \equiv a_{In} + ja_{Qn}$ is the data symbol from complex plane ($a_n = \sqrt{2}/2(\pm 1 \pm j)$ for QPSK/OQPSK signaling). T is the symbol interval, f is the carrier frequency offset, and τ is the delay factor that is 0 for QPSK and 0.5 for OQPSK. The matched filter for an optimal receiver can be modeled as [1] shown in Figure 1. $y(t)$ is down

converted by carrier frequency offset estimate \hat{f} , and then sampled at rate of $1/T_s$, typically $T = MT_s$, with M an integer. The sampled signal is filtered by a matched shaping filter with response $g(-t)$ and timing offset εT . The output is then decimated down to a rate of $1/T$ to obtain a one sample per symbol signal $z(nT + \varepsilon T)$. The demodulator corrects the phase offset θ and timing offset ε of $z(nT + \varepsilon T)$ prior to making symbol decisions and recovering the transmitted symbol \hat{a}_n . $z(nT + \varepsilon T)$ is given by:

$$z(nT + \varepsilon T) = \sum_{k=-\infty}^{\infty} y(kT_s) e^{-j(2\pi f k T_s)} g_{MF}(nT + \varepsilon T - kT_s) \quad (2)$$

2.1. Carrier Frequency Offset Estimation

Initially suppose we have N $z(nT + \varepsilon T)$ ($n = 0, \dots, N-1$) symbols without frequency rotation and $\underline{a} = [a_0, \dots, a_{N-1}]$ is known in DA case. In order to simplify the presentation, let us assume perfect timing (frequency estimation performance in the presence of random timing offset is shown through simulation), unit-energy pulse ($g(t) \otimes g(-t)$), thus $z(nT + \varepsilon T)$ can be simplified as $z(n, f)$, which can be expressed as:

$$z(n, f) = a_n \exp[j(2\pi f n T + \theta)] + \gamma_n \quad (3)$$

where γ_n is additive Gaussian noise. Correlation method is adopted to remove data modulation a_n , let

$$r_n \equiv z(n, f) a_n^* = E_s \exp[j(2\pi f n T + \theta)] + \gamma_n a_n^* \quad (4)$$

It is easy to show that the autocorrelation of the exponential wave is still an exponential wave at high SNR (simulation shows that high SNR condition is not necessary), i.e.,

$$\begin{aligned} R(m) &\equiv \frac{1}{N-m} \sum_{n=m}^{N-1} r_n r_{n-m}^* \\ &= E_s^2 \exp[j(2\pi f m T)] + \text{noise}(m) \end{aligned} \quad (5)$$

where $m = 1, \dots, L$ ($L < N-1$). Mengali [4] proposed a frequency estimator based on modeling noise(m) and the work done by Kay [2]. From simulation we find that for N large enough noise(m) can be approximated as white Gaussian noise. The sequence $\{R(m)\}$ can be treated as a continuous wave (with frequency f) which is passed through a noise removal process. At high SNR, many good frequency estimation methods have been derived. Kay [2] presented a frequency estimation method based on weighted sum of phase difference. His frequency estimator is ML at high SNR. Let us define the following process:

$$\theta(m) = \arg[R(m)], \quad m = 1, \dots, L \quad (6)$$

and

$$\Delta_m = \begin{cases} \theta(1), & m = 0 \\ (\theta(m+1) - \theta(m)) \bmod(2\pi), & 1 < m < L \end{cases} \quad (7)$$

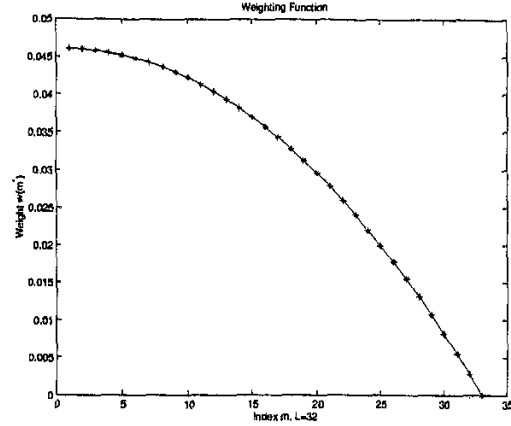


Figure 2: Weighting Function $\{w_m^*\}$

We borrow from Kay's frequency estimator, that is the weighted sum of phase difference. Because $R(m_1)$ is calculated based on more data than $R(m_2)$ when $m_1 < m_2$, after some arithmetic we derived the following carrier frequency offset estimator:

$$\hat{f} = \frac{1}{2\pi T} \sum_{m=0}^{L-1} w_m^* \Delta_m \quad (8)$$

where

$$w_m^* = \frac{3((2L+1)^2 - (2m+1)^2)}{((2L+1)^2 - 1)(2L+1)}, \quad m = 0, \dots, L-1 \quad (9)$$

The weighting function is shown in Figure 2. It is easy to see that the weight w_m^* decreases as m increases. That is because as m gets larger and larger, the number of terms used to compute $R(m)$ reduces and thus makes Δ_m less and less accurate. Compared with Mengali's algorithm, our estimator adopts different weighting function, L can be less than $N/2$ (e.g. when $N = 96$, $L = 32$ can achieve the CRLB at 0dB).

2.2. Joint Carrier Phase and Timing Offsets Estimator

Assuming zero frequency offset estimation error, there are K ($K = MN$) observations of $z(kT_s + \varepsilon T)$ ($k = 0, \dots, K-1$) available for estimating ε and θ , $\varepsilon \in [-0.5, 0.5]$. According to the work done in [1], the maximization object function of ML joint phase and timing offsets estimation in AWGN channel is

$$L(\underline{a}, \varepsilon, \theta) = C \exp \left\{ -\text{Re} \left[\sum_{n=0}^{N-1} a_n^* z(nT + \varepsilon T) e^{-j\theta} \right] \right\} \quad (10)$$

where C is a positive constant and $\underline{a} = [a_0, \dots, a_{N-1}]$ which is the data pattern and is known to the estimator. Let us define

$\mu(\varepsilon)$ as:

$$\mu(\varepsilon) = \sum_{n=0}^{N-1} a_n^* z(nT + \varepsilon T) \quad (11)$$

The ML joint phase and timing estimator is given by [1]:

$$\hat{\varepsilon} = \arg \max_{\varepsilon} |\mu(\varepsilon)| \quad (12)$$

$$\hat{\theta} = \arg[\mu(\hat{\varepsilon})] \quad (13)$$

According to the Equivalence Theorem [1], and assuming that $c(t)$ and $f(t)$ are all-pass filters, $z(nT + \varepsilon T)$ is equivalent to the following:

$$z(nT + \varepsilon T) = \sum_{k=0}^{N-1} a_k r(nT + \varepsilon T - kT) e^{-j\theta} + N_n \quad (14)$$

where

$$r(t) = g_T(t) \otimes g_T(-t) = \frac{\sin(\pi t/T) \cos(\alpha \pi t/T)}{\pi t/T \sqrt{1 - 4\alpha^2 t^2/T^2}}$$

The above expression also assumes that raised cosine shaping is adopted with α denoting the rolloff factor. N_n is the sampled version of $n(t)$, Gaussian noise, after being filtered by $g_{MF}(t)$.

Arriving at a solution to eq. (12) is a difficult task and the resulting hardware structure presented in [1] is quite complicated. It is well known that a quadratic form can be used to approximate the central segment of a convex function around its peak. The expression for $\mu(\varepsilon)$ can be approximated by a quadratic equation as shown below. If $\varepsilon \rightarrow 0$, the inter-symbol-interference (ISI) and noise N_n can be ignored and we can simplify $|\mu(\varepsilon)|$ as

$$|\mu(\varepsilon)| \approx E_s \sum_{n=0}^{N-1} |a_n|^2 r(\varepsilon T) = N E_s r(\varepsilon T) \quad (15)$$

where $|a_n|^2 = 1$ ($n = 0, \dots, N-1$). Furthermore by letting $t = \varepsilon T$ and using Taylor series approximations for sine and cosine functions and after some simplification, we arrive at

$$|\mu(t)| \approx N E_s \left(1 - \frac{\pi^2 t^2}{6T^2} \right) \quad (16)$$

Figure 3 shows the result of numerical evaluation of $|\mu(\varepsilon)|$ which follows a quadratic form. From eq. (16) we can use a second order polynomial to approximate the relationship between sampling time and the magnitude of correlation $|\mu(t)|$ given that these sampling points are close enough to the ideal sampling point (i.e. t is close enough to 0). Using a general form of the second order polynomial

$$|\mu(t)| = b_2 t^2 + b_1 t + b_0 \quad (17)$$

suggests that a joint phase and timing estimator can be derived based on three adjacent samples of $|\mu(t)|$. These samples are

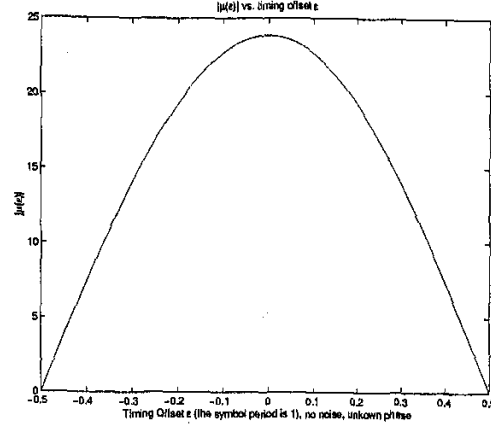


Figure 3: Correlation Magnitude $|\mu(\varepsilon)|$ vs. Timing Offset ε

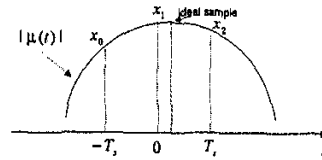


Figure 4: Three Sampling Points Model

the closest ones to the ideal sampling point as shown in Figure 4. In order to meet the condition that t is close enough to 0, two measures are adopted: one is that the sampling rate M (samples per symbol) is large enough (simulation shows that $M = 4$ can achieve good performance); second is locating the largest available magnitude x_1 through peak search. Let us define the sampling time of x_1 as nominal 0 on time axis. Therefore the sampling times of x_0 and x_2 are $-T_s$ and T_s , respectively. A *LaGrange* interpolating polynomial can be adopted based on the values of x_k ($k = 0, 1, 2$):

$$\begin{aligned} |\mu(t)| &= \sum_{k=0}^2 x_k \prod_{i=0, i \neq k}^2 \frac{t - t_i}{t_k - t_i} \\ &= b_2 t^2 + b_1 t + b_0 \end{aligned} \quad (18)$$

using the fact that $t_0 = -T_s$, $t_1 = 0$, $t_2 = T_s$, we can get

$$b_2 = \frac{1}{T_s^2} \left(\frac{x_0}{2} - x_1 + \frac{x_2}{2} \right) \quad (19)$$

$$b_1 = \frac{1}{T_s} \left(\frac{x_2}{2} - \frac{x_0}{2} \right) \quad (20)$$

$$b_0 = x_1 \quad (21)$$

The ML timing offset estimator (12) is the $\hat{\varepsilon}$ which maximizes $|\mu(\varepsilon)|$. It is easy to compute the sampling time of the peak of

$|\mu(t)|$ from a second order polynomial, i.e.

$$t_{peak} = -\frac{b_1}{2b_2} = \frac{(x_0 - x_2)T_s}{2x_0 - 4x_1 + 2x_2} \quad (22)$$

therefore, the ML estimate of ε is

$$\hat{\varepsilon} = -\frac{t_{peak}}{T} = \frac{x_2 - x_0}{M(2x_0 - 4x_1 + 2x_2)} \quad (23)$$

The phase estimator is shown in eq. (13). Interpolation techniques can be applied to correct the timing offset before phase estimation. This however introduces an additional delay in the demodulation process. Simulations show that using the time for the non ideal sample of x_1 is sufficient for meeting the CRLB (sampling time of x_1 is t_1). This leads to

$$\hat{\theta} = \arg[\mu(t_1)] \quad (24)$$

In order to locate the largest available value x_1 easily, a highly correlated data pattern \underline{a} is selected. [6] discusses this problem in depth. Here unique word (UW) and alternating (one zero) data patterns are investigated.

3. VLSI IMPLEMENTATIONS

For the frequency estimator, the calculation of $R(m)$ (eq. (5)) is a hardware intensive task that requires $(2N - L - 1)L/2$ complex multiplication and $(2N - L - 3)L/2$ additions. In order to make full use of each input data and exploit concurrency, we propose the systolic VLSI implementation as shown in Figure 5. If higher speed clock is available, the complex multipliers can be shared on time division basis. $\{R(m)\}$ will be available on the clock cycle following the one latching the N th data symbol into the estimator. Frequency offset can then be calculated via eq. (8). One advantage of this structure is that it is scalable. If we want to increase L to get a better performance, more elements can be added at the right hand side shown in Figure 5.

The hardware block diagram for the joint phase and timing estimator is shown in Figure 6. The multi-sample correlator generates outputs at a higher rate than one sample per symbol. A systolic VLSI implementation of the correlator is shown in Figure 7, where x_{ij} denotes the i th symbol ($i = 0, \dots, N - 1$), j th sample ($j = 0, \dots, 3$) of the output from the matched shaping filter. In QPSK case, $a_n = \pm 1 \pm j$, only adders are necessary therefore the computational complexity is relatively small especially when using the correlator as soft-decision UW detector. Through peak search module, we can locate x_0 , x_1 and x_2 . An ArcTan Lookup table (LUT) is used when estimating the phase offset.

4. PERFORMANCE BOUNDS AND SIMULATION RESULTS

The performance lower bound for unbiased ML estimation is the Cramer-Rao lower bound (CRLB). The CRLB_{DA} for DA

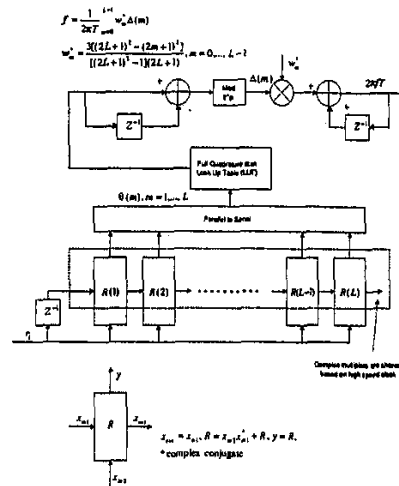


Figure 5: Systolic VLSI Structure of Carrier Frequency Offset Estimator

frequency estimation is given by [9] as follows:

$$E[(fT - \hat{f}T)^2] \geq 6 \left\{ 4\pi^2 \frac{E_b}{N_0} N(N^2 - 1) \right\}^{-1} \quad (25)$$

The CRLB_{DA} for phase estimation is given by [9] as follows:

$$E[(\theta - \hat{\theta})^2] \geq \left\{ \frac{2E_b}{N_0} N \right\}^{-1} \quad (26)$$

Moeneclaey proposed the CRLB for i.i.d. random data pattern (i.e., no information about \underline{a} available) in [7]. The bound for the case where the sampling rate $1/T_s \geq 2B$ (B is the bandwidth of $r(t)$) and N large enough is given by

$$E[(\tau - \hat{\tau})^2] \geq T^2 \left\{ \frac{2E_b}{N_0} N \int 4\pi^2 f^2 \mathcal{R}(f) df \right\}^{-1} \quad (27)$$

with $\mathcal{R}(f)$ the Fourier transform of $r(t)$. Jiang has proposed the following expression for CRLB_{DA} in [6]:

$$\left\{ \frac{2E_b}{N_0 NT} \left[\sum_{k=-K/2}^{K/2-1} \left(\frac{2\pi k}{N} \right)^2 \mathcal{R} \left(\frac{k}{NT} \right) |\mathcal{A}[k]|^2 \right] \right\}^{-1} \quad (28)$$

where $\mathcal{A}[k]$ is the k th element of N -point discrete Fourier transform (DFT) of \underline{a} , i.e. $\mathcal{A}[k] = \sum_{n=0}^{N-1} a_n e^{-j(2\pi nk/N)}$. According to eq. (28), CRLB_{DA} has different values for different data patterns. Two data patterns have been investigated: alternating one-zero pattern (i.e. $a_i = (-1)^i \sqrt{2}/2(1 + j)$), and a unique word pattern. A 48-symbol UW was selected. According to eq. (28) for the alternating one-zero data pattern

$$\text{CRLB}_{\text{DA}}|_{10} = \left\{ 2\pi^2 \frac{E_b}{N_0} N \right\}^{-1} \quad (29)$$

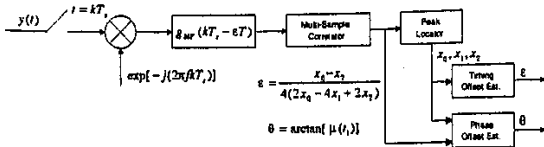


Figure 6: Joint Carrier Phase and Timing Offsets Estimator

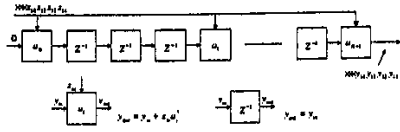


Figure 7: Multi-Sample Correlator

and thus the performance is independent of rolloff factor α given that $\alpha > 0$. For the UW pattern, the timing estimation $CRLB_{DA}$ is closely related to the rolloff factor. It follows from eq. (28) that the larger the rolloff factor, the smaller $CRLB_{DA}$. Figure 8 shows eq. (28) plotted as a function of SNR for three different values of rolloff factor.

The parameters for the computer simulations were QPSK signaling, $N = 96$ and $L = 32$ in an AWGN channel for frequency estimation, $N = 48$ and $M = 4$ in the AWGN channel for joint phase and timing estimation. Figure 9 shows normalized root mean squared (RMS) frequency estimation error with $f = 0.13/T$, which is compared with the $CRLB_{DA}$ for frequency estimation. From simulation we can see that the estimation RMS error is very close to the $CRLB_{DA}$ even at 0dB, the performance degradation caused by timing error is very small. Figure 10 shows the saw tooth characteristics of eq. (23) under no noise conditions with random phase. From simulations we can see that (23) is an unbiased estimate of ϵ . Peak search (i.e. locating x_1) resolves the $m/4$ ($m = \pm 1, \pm 2$) ambiguity.

For phase and timing estimation, different rolloff factors for the raised cosine shaping function were also tested. Simulation shows that the RMS timing estimation error meets the $CRLB_{DA}$ of timing estimation for all α s and data patterns. Simulations also support that for the one-zero pattern the RMS timing error is independent of α , while for the UW pattern it decreases as α increases. This is in agreement with the evaluation of the $CRLB_{DA}$. Figure 11 shows the timing offset estimation performance with $\alpha = 0.5$, where one-zero pattern and UW pattern of QPSK are illustrated. Figure 12 shows the phase estimation performance. The RMS phase estimation error meets the $CRLB_{DA}$ for phase estimation.

5. CONCLUSIONS

Simulation shows that the performance of our estimators are very close to the $CRLB_{DA}$ even at 0dB, these algorithms are

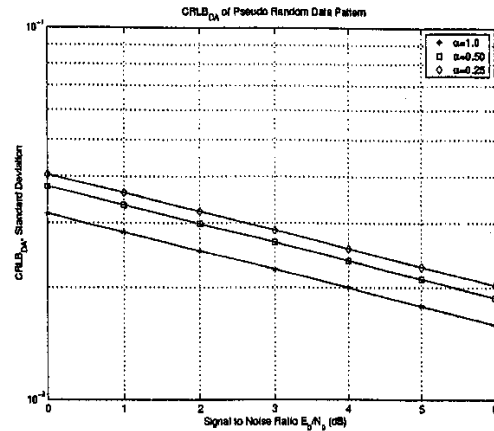


Figure 8: The $CRLB_{DA}$ for Timing Estimation with UW Pattern

good approximations of the ML estimations since if the performance of an unbiased estimation meets the CRLB then the estimation is ML [5]. The techniques proposed here can be used in high performance PSK burst modems working under large carrier frequency offset and low SNR conditions. The complexities of these algorithms are moderate.

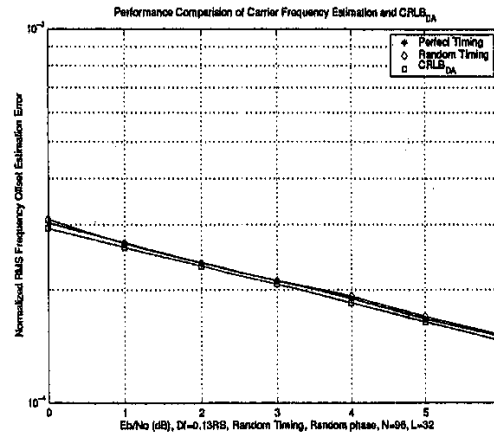


Figure 9: RMS Carrier Frequency Offset Estimation Error vs. $CRLB_{DA}$

6. REFERENCES

- [1] H. Meyr, M. Moeneclaey, S. Fechtel, *Digital Communication Receivers, Synchronization, Channel Estimation, and Signal Processing*, New York: Wiley, 1998.

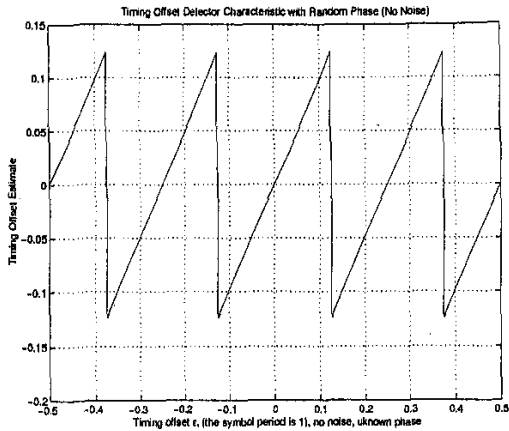


Figure 10: Timing Offset Estimate $\hat{\epsilon}$ vs. Timing Offset ϵ

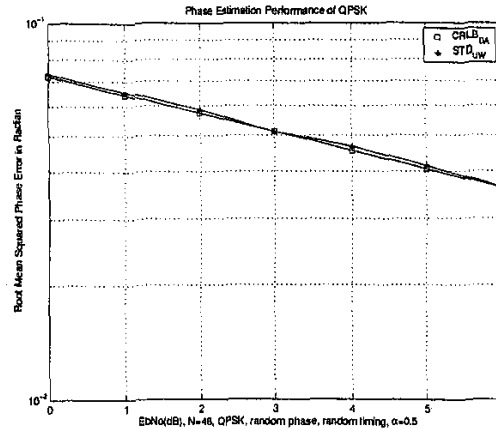


Figure 12: Phase Offset Estimation Performance (UW pattern, $\alpha = 0.5$)

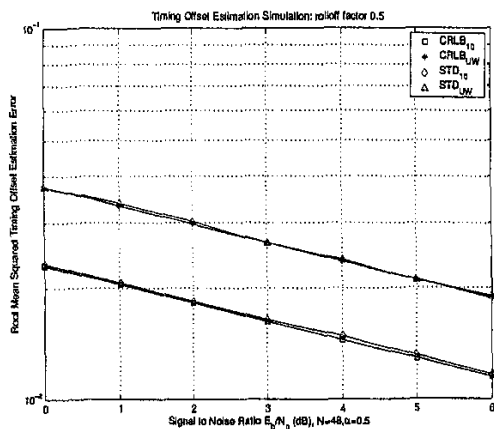


Figure 11: Timing Offset Estimation Performance (one zero pattern vs. UW pattern, $\alpha = 0.5$)

- [2] S. Kay, "A Fast and Accurate Single Frequency Estimator", *IEEE Trans. Acoust., Speech, Signal Processing*, vol. 37, no.12, pp.1987-1990, December 1989.
- [3] Y. Jiang, W. Ting, F. Verahrami, R. Richmond, J. Baras, "A Carrier Frequency Estimation Method of MPSK Signals And Its Systolic VLSI Implementation", *Proc. CISS 99*, Jan., 1999.
- [4] U. Mengali, M. Morelli, "Data-Aided Frequency Estimation for Burst Digital Transmission", *IEEE Trans. Comm.*, vol. 45, no. 1, pp.23-25, Jan. 1997.
- [5] H. L. Van Trees, *Detection, Estimation and Modulation Theory, Part I*, New York: Wiley, 1968.

- [6] Yimin Jiang, John S. Baras "Maximum Likelihood Estimation of Timing Offset: A Frequency Domain Approach", to appear.
- [7] C. Georghiades, M. Moeneclaey, "Sequence Estimation and Synchronization from Nonsynchronized Samples", *IEEE Trans. Inform. Theory*, vol. IT-37, pp. 1649-1657, Nov. 1991.
- [8] H. T. Kung, "Why Systolic Architecture", *IEEE Computer*, vol. 15, no. 1, pp. 37-46, Jan. 1982.
- [9] D. Rife, R. Boorstyn, "Single-Tone Parameter Estimation from Discrete-Time Observations", *IEEE Trans. Info. Theory*, vol. IT-20, no. 5, pp. 591-598, Sept. 1974.